Applied Catalysis B: Environmental 136–137 (2013) 160–167

Contents lists available at SciVerse ScienceDirect

Applied Catalysis B: Environmental

journal homepage: www.elsevier.com/locate/apcatb

Pt-Cu electrocatalysts for methanol oxidation prepared by partial galvanic replacement of Cu/carbon powder precursors

I. Mintsouli[a], J. Georgieva[b], S. Armyanov[b], E. Valova[b], G. Avdeev[b], A. Hubin[c], O. Steenhaut[c], J. Dille[d], D. Tsiplakides[a,e], S. Balomenou[e], S. Sotiropoulos[a,*]

[a] Department of Chemistry, Aristotle University of Thessaloniki, Thessaloniki 54124, Greece
[b] Rostislaw Kaischew Institute of Physical Chemistry, Bulgarian Academy of Sciences, Sofia 1113, Bulgaria
[c] Department of Electrochemical and Surface Engineering, Vrije Universiteit Brussel, 1050 Brussels, Belgium
[d] Ecole Polytechnique de Bruxelles, Service 4 MAT Materials, Engineering, Characterization, Synthesis & Recycling, 1050 Brussels, Belgium
[e] Chemical Process Engineering Research Institute, The Centre for Research and Technology Hellas, 570 01, Thermi, Thessaloniki, Greece

ARTICLE INFO

Article history:
Received 13 September 2012
Received in revised form 22 January 2013
Accepted 28 January 2013
Available online 15 February 2013

Keywords:
Platinum catalysts
Galvanic replacement
Binary catalysts
Methanol oxidation

ABSTRACT

A bimetallic Pt-Cu carbon-supported catalyst (Pt(Cu)/C) has been prepared by a room temperature two-step procedure involving the chemical reduction of Cu ions by sodium borohydride in the presence of Vulcan XC72R carbon powder, followed by the partial galvanic replacement of Cu particle layers by Pt, upon immersion in a chloroplatinate solution. The characterization of the Pt(Cu)/C catalyst by XRD has proven the formation of a Pt–Cu alloy while cyclic voltammetry in deaerated acid revealed similar characteristics to those of pure Pt. These two findings point to the existence of Pt-rich outer layers and a Pt–Cu core. The electrocatalytic activity of the bimetallic Pt(Cu)/C catalyst towards methanol oxidation is comparable to or better than that of a commercial 20% Pt Vulcan XC72R catalyst (when assessed by voltammetric or prolonged chronoamperometric experiments respectively). This is attributed to the effect of Cu on CO poison adsorption and removal from Pt. Moreover, related to the same effect but also to the reduced Pt loading of the mixed Pt–Cu particles, the specific mass activity of the prepared catalyst is superior to that of the commercial catalyst.

1. Introduction

In order to increase the intrinsic activity and lower the cost of fuel cell catalysts that are based on precious metals, various carbon-supported multi-metallic catalysts have been developed. The most common preparation routes involve metal ion impregnation or metal oxide precipitation on carbons followed by chemical reduction (either in liquid phase or in a hydrogen atmosphere) [1–3]. Conversely, the preparation of colloidal metal particles (either by the Bonnemann [4] or microemulsion [5] methods) and their subsequent/concurrent adsorption on carbon are also used.

With a primary goal the reduction of precious metal loading, a new method for the preparation of multi-metallic catalysts has been proposed, based on the spontaneous replacement of a metal (M) by a more noble one (e.g. Pt); this is essentially a galvanic replacement process, known also as transmetalation [6]. Adzic and co-workers [7–9] applied it first to the complete replacement of Cu UPD monolayers by Pt, Pd or Ag and then by a series of noble metals or their mixtures (see Ref. [6] and References therein). Kokkinidis et al. applied the technique to the partial replacement of Ti surface layers [10,11] or Cu and Pb polylayers [12,13] by Pt, resulting in the latter case in Pt shell–Cu (or Pb) core particles, denoted as Pt(Cu) or Pt(Pb). Sotiropoulos and co-workers expanded the method to the replacement of Pb, Cu, Fe, Co, Ni polylayers by Pt and Au [14–21].

Until recently, most of work on catalysts prepared by transmetalation has been in search of efficient oxygen reduction electrocatalysts, with only few papers dealing with methanol oxidation in acid. The latter is the fuel reaction in direct methanol fuel cells (see for example Refs. [22,23]) for which Pt-based catalysts, tolerant to CO intermediate poisoning, have been sought for many years, either by ad-atom adsorption or alloy formation [24–31]. Sotiropoulos and co-workers studied methanol oxidation on Pt(Pb) [14] and Pt(Cu), Pt(Ni), Pt(Co) [20] electrodes prepared by transmetalation, where the non-noble metal had been electrodeposited onto glassy carbon substrates. Results on practical high surface area supports such as carbon powders or nanotubes have recently appeared too for PtRu(Pb) [25], PtRu(Co) [26], PtRuCu [27] and Pt(Ag) [28]. Systematic studies of the effect of the third metal, M, to Pt properties (apart from the well-established synergistic effect of Ru) are still needed before advancing the state of the art Pt–Ru materials to improved Pt-Ru-M catalysts. There have been few papers for methanol oxidation on Pt(Cu) supported on carbon powder, where

* Corresponding author. Tel.: +30 2310 997742; fax: +30 2310 443922.
E-mail addresses: eczss@chem.auth.gr, eczss@otenet.gr (S. Sotiropoulos).

0926-3373/$ – see front matter © 2013 Elsevier B.V. All rights reserved.
http://dx.doi.org/10.1016/j.apcatb.2013.01.059

the Cu precursor was electrodeposited on carbon and Pt was in excess [29,30] as well as a short communication of Pt(Cu) hollow nanocrystals showing some electrochemical evidence for increased catalytic activity [31].

Following our recent finding that model Pt(Cu) electrodes, prepared by transmetalation of Cu layers on glassy carbon, exhibited higher medium-term activity towards methanol oxidation [20], the aim of the work presented here has been the establishment of the two-step method as an alternative route for the preparation of practical Pt(Cu) methanol oxidation catalysts. Specific objectives have been: (i) the formation of Pt(Cu) particles on the fuel cell technology standard of Vulcan XC72R carbon, C, via the partial galvanic replacement of Cu/C precursor particles formed by chemical reduction of copper ions; (ii) the microscopic (TEM), spectroscopic (EDS, XPS) and crystallographic (XRD) characterisation of the Pt(Cu)/C catalyst; (iii) the electrochemical characterisation of Pt(Cu)/C by means of H adsorption/desorption and CO monolayer oxidation and (iv) the comparative voltammetric and chronoamperometric study of methanol oxidation on electrodes prepared by the Pt(Cu)/C catalyst and a commercial Pt/C catalyst.

2. Experimental

2.1. Preparation of Cu/C and Pt(Cu)/C powder catalysts and electrode preparation

To increase the number of functional groups on the Vulcan XC72R (Cabot) carbon powder support (hence its metal ion adsorption affinity too) it was subjected to an oxidative pre-treatment according to Ref. [25]. 0.25 g of carbon black was immersed in 100 ml solution of 1.0 M sulfuric acid (Aldrich, puriss) and 10 g of ammonium persulfate (Merck, ACS reagent) at room temperature and stirred for 24 h using a magnetic stirrer. The suspension was filtered, the precipitate was rinsed with pure H_2O and left to dry overnight. The oxidized carbon was mechanically grinded in a mortar and suspended in 90 ml water. 0.4 g $CuSO_4{\cdot}5H_2O$ (0.1 g Cu or 0.0016 g-atom of Cu; Sigma–Aldrich (ACS reagent)) was dissolved in 10 ml water and added to the suspension. The suspension was left for 24 h under magnetic stirring to ensure maximum copper ion adsorption on the carbon surface. In order to reduce Cu(II), 12.8 ml (0.0128 mol) of 0.1 M $NaBH_4$ in 1 M NaOH solution were added to the suspension (the reducing agent was added in excess). The suspension was stirred in an ultrasonic bath for 30 min and filtered. The obtained Cu/C precipitate was left to dry in air.

0.140 g of the as prepared Cu/C powder catalyst were added slowly under continuous magnetic stirring to 50 ml of a 10^{-3} M K_2PtCl_6 (Sigma–Aldrich, ACS reagent, ≥37.50% as Pt) in 0.1 M HCl (Aldrich) solution and then was transferred to an ultrasonic bath for 45 min. Electroless deposition of Pt with concurrent galvanic (partial) replacement of Cu occurred:

$$2Cu + PtCl_6^{2-} \rightarrow Pt + 2Cu^{2+} + 6Cl^{-}, \quad (1)$$

as expected from the positive sign of the $E_{PtCl_6^{-2}/Pt} - E_{Cu^{2+}/Cu}$ standard potential difference [32], indicated by the colour difference between the filtrate of the treated Cu/C suspension (light blue) and the chloroplatinate reactant solution used (yellow) and confirmed by the results of EDS analysis that show the existence of both Pt and Cu in the catalyst (see Section 2.2 below).

For the electrochemical testing of the catalyst, 3 mg of the thus prepared Pt(Cu)/C material (or of commercial 20% (w/w) Pt/C catalyst, ETEK) were suspended in 0.5 ml methanol together with drops of a Nafion® (protonic form) 5% (w/w) solution in a mixture of low aliphatic alcohols and 45% water (Aldrich), amounting to 2.5 mg of Nafion® polymer. The as prepared suspension was homogenized in an ultrasonic bath and a given quantity of the slurry (containing the desired catalyst weight in the 0.2–0.4 mg range) was placed in a drop-wise manner on a flat glassy carbon electrode (GC, BAS Inc.) over a total area of 0.385 cm^2 and left to dry (resulting in a total catalyst loading in the 0.5–1.0 mg cm^{-2} range). The exact weight of added polymer and catalyst for each electrode was determined with the help of an electronic balance, during parallel additions of the corresponding solution and slurry on an aluminum foil until solvent evaporation was complete and no further weight change was observed. Based on the analysis of the catalysts by EDS (see Section 3.1 below) the Pt loading for the electrodes tested was 0.05 mg cm^{-2} for the Pt(Cu)/C catalyst and 0.18 mg cm^{-2} for the Pt/C ETEK catalyst.

2.2. Microscopic, spectroscopic and crystallographic characterisation of the catalysts

Transmission electron microscopy (TEM) was carried out using a Philips M20 TEM system. Energy dispersive spectroscopic (EDS) elemental analysis was performed using the utility of a JEOL 6390/INCA Oxford Energy 350 EDS system. All EDS measurements were made under conditions appropriate for powder samples. The latter were prepared by filling with powder small cylinder microvessels (of a 3 mm diameter and 1 mm depth) made of Al foil. The powder was then pressed by a pestle. Areas about several square microns were probed (typically of the order of 100 μm^2). Several regions (at least 3 for each sample) were probed and the variations in metal content were within the estimated margin of error (see below).

X-ray diffraction patterns of the catalyst powders were obtained using a Philips automatic powder diffractometer (Bragg–Brentano arrangement, fixed slit mode), utilizing Cu Kα filtered radiation (λ = 1.5406 nm) and scintillation registration, with a constant scanning step $\Delta(2\theta) = 0.02^\circ$, and a counting time per step of 3 s.

X-ray photoelectron spectroscopy (XPS) studies were performed in a PHI model 1600 system equipped with an Omni Focus Lens III using a standard Mg Kα X-ray source at a high voltage of 15 kV, 300 W. The PHI Multipak 8 software was used for data interpretation. Since the samples were highly conducting, minimum charging effects were expected; nevertheless, for high resolution spectra the carbon peak was recorded too and used for corrections by setting the carbon peak at 284.4 eV and then using the system's "Autoshift" operation.

2.3. Electrochemical characterisation of coatings

Voltammetric and chronoamperometric experiments were carried out with the Autolab 100 (EcoChemie) system using a Pt wire counter electrode and a Saturated Calomel Electrode (SCE; Radiometer), in three-compartment cells with the counter and reference electrode chambers separated from the working electrode chamber by a glass frit and a lugin capillary respectively.

The electrode was first treated in a deaerated 0.1 M $HClO_4$ solution where it was scanned between the hydrogen and oxygen evolution potential limits at the fast potential scan rate of 500 mV s^{-1} until a steady state voltammogram was obtained. This was attained typically after 10–20 cycles (during which decreasing anodic currents due to uncovered Cu particles were recorded) and remained unchanged after as many as 150 cycles. Following that, the electrochemically treated electrode was scanned again in a fresh deaerated 0.1 M $HClO_4$ solution at a lower scan rate of 10 mV s^{-1} until a steady state voltammogram (similar to that expected for pure Pt) was attained. This was achieved after 2–3 cycles. Then, the solution was saturated with pure CO gas (>99.99% purity; Air Liquide) and the Pt(Cu)/C/GC electrode was held at +0.10 V vs. SCE for 5 min (allowing for CO adsorption), before scanned to more positive potentials at a 50 mV s^{-1} potential sweep

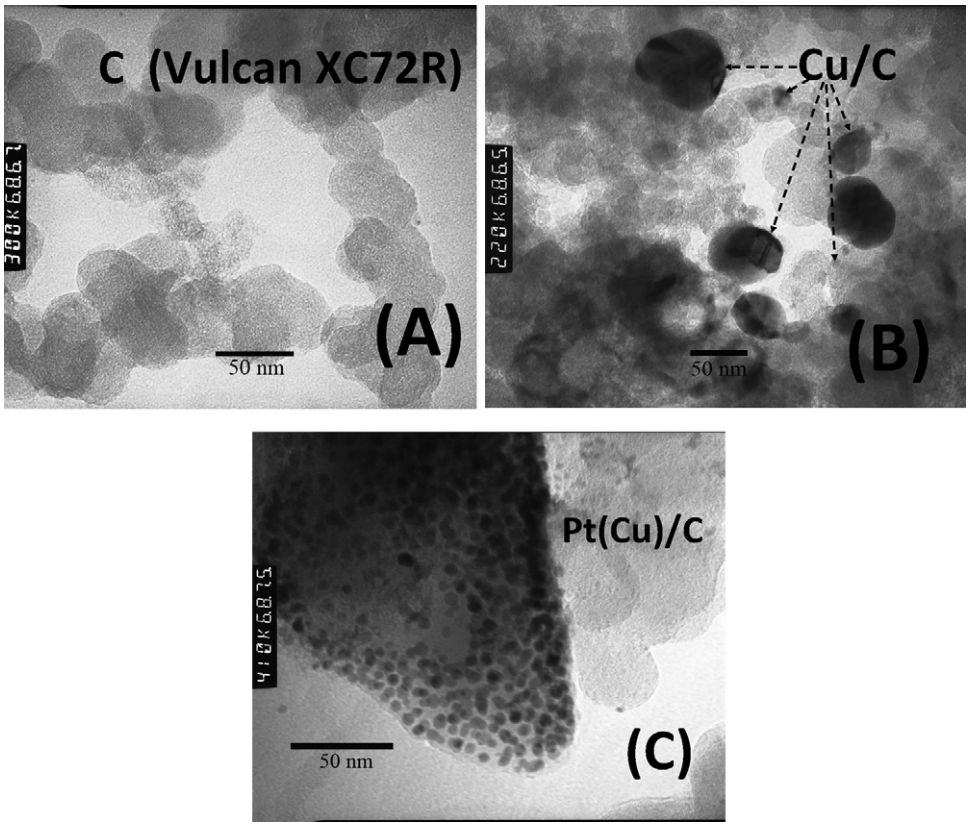

Fig. 1. TEM micrographs of: (A) Vulcan XC72R carbon particles; (B) Cu/C particles prepared by chemical reduction of Cu(II) ions by a 0.1 M $NABH_4$ + 1 M NaOH solution; (C) Pt(Cu)/C catalyst particles prepared by galvanic replacement during immersion of the Cu/C material in a 0.1 M HCl + 10^{-3} M K_2PtCl_6 solution.

rate, for CO monolayer oxidation. Finally, the solution was replaced by a 0.1 M $HClO_4$ + 0.5 M CH_3OH deaerated solution (Riedel; puriss p.a., ACS reagent, ≥70% and Chromasolv® for HPLC, gradient grade, ≥99.9% respectively) and the electrode was swept at a 5 mV s^{-1} between +0.10 V and +0.80 V vs. SCE, until a steady-state voltammogram was obtained (typically for 2–4 times); it is the forward (positive-going) scan of the steady-state response that is presented here.

During medium-term constant potential experiments of 300 s, the potential was kept at +0.40 V or +0.50 V vs. SCE in a 1 M $HClO_4$ + 0.5 M CH_3OH deaerated solution, following a conditioning potential protocol. The latter involved initial contact with the solution at −0.30 V vs. SCE for 2 s (where methanol oxidation is minimum), a step to +0.50 V vs. SCE for 2 s (for desorption of adsorbed H and oxidation of CO being formed by methanol oxidation at this potential) and a stay at 0.00 V for 2 s (in the double layer region).

3. Results and discussion

3.1. Microscopic, spectroscopic and crystallographic characterisation of Cu/C and Pt(Cu)/C powders

Fig. 1 shows the TEM micrographs of the carbon powder support (A), the Cu/C catalyst (B) and the platinised Pt(Cu)/C composite (C). The carbon support consists of 30 nm spherical particles that are further aggregated in chain-like structures. The copper particles indicated in Fig. 1(B) have a wide range of dimensions (ranging from few nm to tens of nm), with the larger particles consisting of polyhedral crystals. The Pt(Cu) particles resulting from the immersion of the precursor Cu/C in a chloroplatinate solution according to reaction (1) have a much narrower size distribution and much smaller size (in the 3–5 nm range). This indicates that large quantities of Cu (especially those organised at large particles) are not contained in the final catalyst, either because they collapse-loose adhesion to the carbon substrate (due to a non-homogeneous exchange–dissolution process) or/and because they are etched away by a competitive process (oxygen reduction from the non-dearated acidic chroroplatinate solution).

EDS analysis of the Cu/C and Pt(Cu)/C catalysts of the batch of the sample shown in Fig. 1 gave a 27.7 ± 0.95% (w/w) Cu content (with 65.2% C and 7.1% O) for the former and a 2.7 ± 0.05% (w/w) Cu–9.5 ± 0.25% (w/w) Pt composition for the latter (its analysis gave also 82.3% C and 5.5% O). The errors correspond to 2σ values estimated by standardless analysis based on standards included in the software of JEOL 6390 (according to its manual, when the error in the analysis is over 3 sigma, σ, the measurement is discarded). The Cu–Pt atomic ratio of the catalyst shown in Fig. 1 and used for the electrochemical tests presented could be thus estimated as 47% Cu–53% Pt i.e. 0.89. The Cu–Pt atomic ratio in 6 different catalyst batches prepared was found 1.09 ± 0.22 (within 3σ of the estimated average).

The Cu content of the precursor material is as expected for complete reduction of the Cu(II) ions contained in the peparation solution by the $NaBH_4$ excess (see Section 2.1 above). Based on the elemental composition of the Cu/C and Pt(Cu)/C materials, the 2–1 Cu–Pt stoichiometry of the exchange reaction of (1) and the actual quantities of the materials used for the preparation, we can estimate that only 9.3% of Cu originally present in the deposit remains in the final product, 19.0% has been exchanged for Pt whereas 71.7% has been "lost" in the exchange solution. This, together with the TEM pictures discussed above, confirms and quantifies the collapse of large-partially platinized Cu particles as well as the further dissolution of uncovered Cu, coupled with oxygen reduction in the acidic environment. Regarding the competition between Pt(IV) and

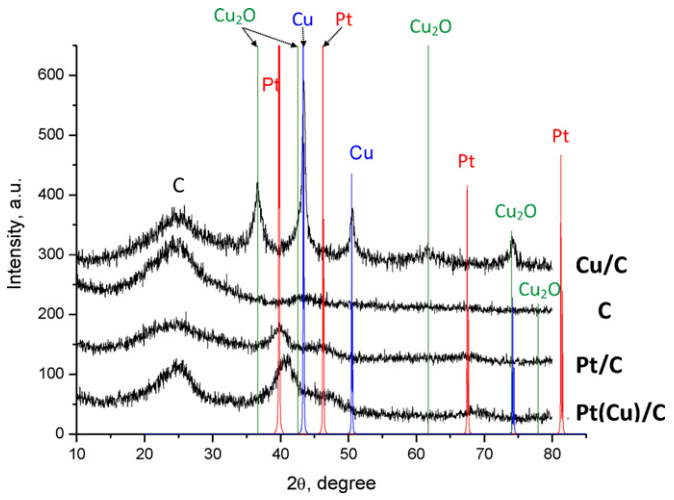

Fig. 2. XRD diffractograms of Vulcan XC72R C, Pt/C (ETEK) and Cu/C, Pt(Cu)/C particles prepared by chemical reduction and galvanic replacement respectively.

oxygen reduction (the cathodic processes coupled with Cu dissolution), one should note that they are both expected to have very fast kinetics since the exchange reaction rate depends on the difference between the the standard potentials of the couples involved in the two processes ($E_{PtCl_6^{-2}/Pt} - E_{Cu^{n+}/Cu}$ and $E_{O_2/H_2O} - E_{Cu^{2+}/Cu}$) [14,20] and both cathodic half-reactions have a high standard potential with respect to that of Cu (+0.744 V vs. SHE for $Pt(IV)Cl_6^{2-}/Pt$, +1.23 V vs. SHE for O_2/H_2O and +0.340 V vs. SHE for Cu^{++}/Cu [32]). Therefore, the exchange process is expected to be under mass transfer control at all times in an unstirred solution. Given the fact that the concentration of oxygen in air-equilibrated solutions is around 0.25 mM [33] and that of $Pt(IV)Cl_6^{2-}$ used was 1 mM, it follows that in the beginning of the reaction Cu dissolution is coupled with Pt deposition, whereas when Pt is exhausted at longer times Cu corrodes with oxygen reaction taking over. The presence of oxygen in the acidic exchange solution and the resulting etching of any un-protected/non-platinized Cu, makes the use of a second step of catalyst curing in acid (employed in the similar preparation route of Ref. [34]) unnecessary.

Fig. 2 shows the XRD difractograms of carbon support C, the Cu/C precursor the Pt(Cu)/C catalyst and, for comparison, a Pt/C commercial catalyst. All XRD patterns except those for the carbon support correspond to fcc structures. Even the strongest [1 1 1] peak of Pt/C and Pt(Cu)/C is rather broad, suggesting very small crystallite dimensions (using the Scherer formula similar values for crystallite size, ca. 3 nm, were estimated). The most interesting feature of the spectra is the shift of the Pt peak to higher 2θ values (41.08°) with respect to both the literature value for pure Pt (39.76° from JCPDS#04-0802) and that of the plain Pt/C catalyst. From the position of the [1 1 1] peaks at ca. 40°, the lattice parameters of Pt(Cu)/C and Pt/C were calculated as $\alpha_{Pt(Cu)/C}$ = 3.81 Å and $\alpha_{Pt/C}$ = 3.93 Å. The lattice parameters for pure Pt and Cu are given as α_{Pt} = 3.9231 Å and α_{Cu} = 3.6150 Å in JCPDS#04-0802 and JCPDS#04-0836 respectively. The decrease in lattice parameter of the Pt(Cu) system with respect to that of Pt is indicative of the formation of a Pt–Cu alloy, whereby a smaller atom (Cu) enters the lattice of a larger host (Pt). By the application of Vegard's law [35] to the observed shift of the Pt(1 1 1) peak and the corresponding change of the lattice parameter, one can write:

$$\alpha_{Pt(Cu)} = X_{Pt}\alpha_{Pt} + X_{Cu}\alpha_{Cu} = X_{Pt}\alpha_{Pt} + (1 - X_{Pt})\alpha_{Pt} \quad (2)$$

where X_{Pt} and X_{Cu} are the atomic fractions of Pt and Cu in the alloy, and estimate the atomic composition of the Pt–Cu alloy as 63% in Pt and 37% in Cu. The composition of the alloy therefore differs from that of the overall deposit (with a Cu–Pt atomic composition ratio of ca. 1 – see discussion of EDS results above). This, together with the absence of peaks corresponding to pure metallic Pt and Cu, suggests that the remaining quantities of non-alloyed Pt and Cu constitute very small entities (either thin shells or very small pockets) and cannot therefore be detected by XRD. It should be noted however that these are only rough estimates since the quantity of Pt and Cu in the samples is low and the resulting XRD signal quite weak. At this point we should also stress that an accurate description of the state and morphology of the components of such a complex nanoparticulate bimetallic system, based solely on the results of conventional XRD, may be questionable since the XRD pattern obtained characterizes only the predominant crystalline phase (in this case, the alloy) and part of the material (pure Pt and Cu) will not contribute to the diffraction pattern due to the very distorted structure of small nanoparticles [36,37]. Structure characterization of this type of nanoparticulate material is a complex task and apart XRD requires sophisticated analysis by several complementary techniques (HR TEM, optical absorption and Raman spectroscopy [38]).

Another interesting feature of the diffractograms is the existence of Cu oxide peaks in the Cu/C sample which disappear when one passes to the Pt(Cu)/C sample. The existence of Cu oxide peaks for the Cu/C precursor is expected for a sample prepared by Cu(II) reduction in the alkaline $NaBH_4$ solution and its subsequent exposure to atmosphere during a filtration step. The identification of the oxide as Cu_2O or CuO from XRD data requires careful spectra inspection since there is a variety of data available in the JCPDS database literature for both Cu_2O (78-2076, 05-0667) and CuO (78-0420 (currently deleted), 78-0428, 80-1917) and there is significant peak overlapping in some cases. Careful comparison of the position as well as the relative intensity of the recorded peaks with those of the database indicates that the oxides present correspond to Cu_2O. The disappearance of these peaks in the transmetalated Pt(Cu)/C sample (together with the fact that Pt deposition does in fact occur despite the formation of Cu_2O in the precursor) indicates that the oxide is restricted to the outer layers of the Cu core in the Cu/C particles and is etched in the acidic Pt-exchange solution used, revealing areas of metallic Cu that readily react with chloroplatinate according to Eq. (1).

The chemical state and composition of the outer surface layers of the catalyst and its precursor was further probed by XPS. Fig. 3 shows the XPS spectra corresponding to a region of Cu peaks for a Cu/C precursor as received (A) and after Ar-sputtering for 45 s (removing ca. 3 nm of material) (B). Although low signal and quality spectra are obtained in the case of non-sputtered/surface contaminated samples (as also confirmed by very high C peaks-not shown), the broad peak at ca 940 eV is still discernible and point to the presence of oxidized Cu(II) species [39] near the surface, indicating in turn the existence of CuO surface oxides. However, these Cu(II) "satellite" peaks disappear upon mild sputtering (Fig. 3(B)), proving that the CuO film is restricted to the surface of Cu/C particles. The presence of a very thin CuO film over underlying Cu_2O oxides could explain why the former could not be detected by XRD which is not a surface sensitive technique and probes the entire catalyst particle.

Fig. 4(A) shows the same Cu region of the XPS spectra for as received and sputtered Pt(Cu)/C particles of a catalyst batch and the absence of a significant Cu(II) peak suggests that most of the CuO material present on the surface of the Cu/C precursor has been etched by the HCl acid of the chloroplatinate solution (as have the underlying Cu_2O oxides been too-see discussion above). Fig. 4(B) shows a region of the XPS spectrum where peaks attributable to Pt and metallic Cu can be clearly identified. From the XPS spectra shown in Fig. 4, the relative composition of the surface layers with respect to Pt and Cu can be estimated. This, together with bulk

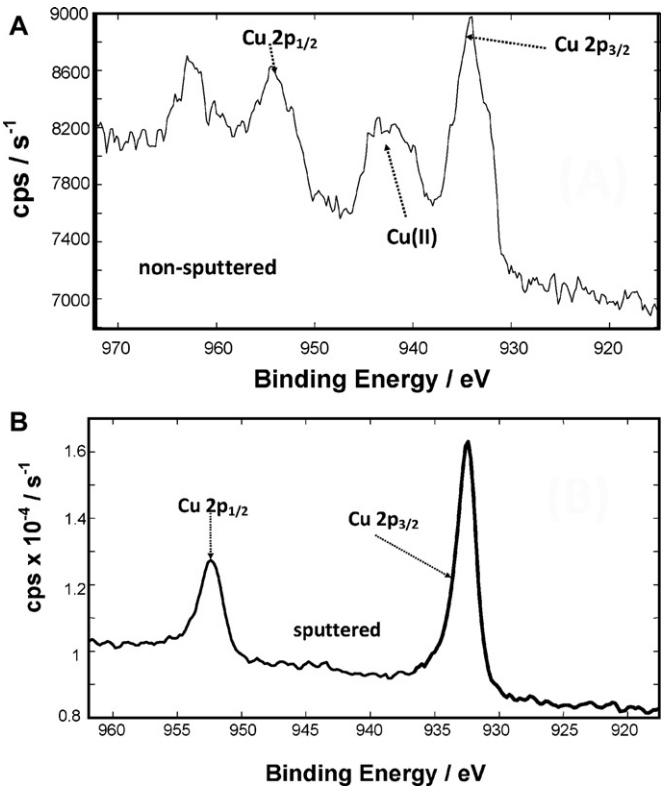

Fig. 3. XPS spectra of Cu/C particles prepared by chemical reduction, (A) before Ar sputter-etching of the surface; (B) after Ar sputter-etching of the surface.

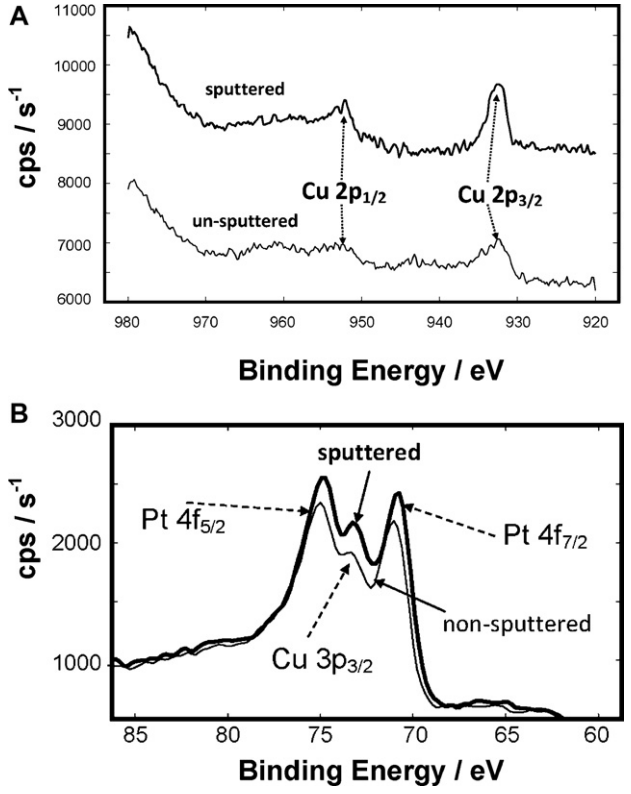

Fig. 4. XPS spectra of non-sputtered and sputtered Pt(Cu)/C particle samples prepared by galvanic replacement, (A) in the Cu2p binding energy region and (B) in the Cu3p and Pt4f binding energy region.

Table 1
Relative atomic percentage composition of Cu and Pt in Pt(Cu)/C catalysts, obtained by XPS and EDS spectroscopy. (Cu content by XPS was determined both for high (Cu2p) and low (Cu3p) binding energy electrons, representative of the surface and the core of the material respectively.).

	$XPS_{surface}$ (Cu2p)	XPS_{core} (Cu3p)	EDS
Cu at%	40	52	56
Pt at%	60	48	44

composition of the sample obtained by EDS, is given in Table 1. The Cu content obtained from the high binding/low kinetic energy Cu(2p) electrons is indicative of the outer surface layers, that obtained from the low binding/high kinetic energy Cu(3p) electrons corresponds to inner surface layers whereas the composition obtained by EDS is representative of the bulk of the material. A careful inspection of these results reveals an increase in Pt content as one moves from the core to the shell of the particles, in complete accordance with an expectation for a Pt-rich shell.

Summarizing, the combination of XRD and XPS data presented above could point to the existence of a thin CuO surface layer on top of thicker Cu_2O underlayers, over a metallic Cu core, in the case of the Cu/C precursor; such a structure has already been proposed for oxidized Cu nanoparticles [40]. Hence, despite many similarities between our preparation procedure and that of Sarkar and Manthiram [34], there is a fundamental difference in that we do have the formation of an intermediate CuO surface film and Cu_2O underlayers whereas they do not. This is because they form their Cu/C in a slightly acidic solution and then they add the chloroplatinate solution to the deaerated slurry (without any intermediate filtration step or oxygen exposure). That procedure probably leads to very fast Pt–Cu exchange rates with non-homogeneous Pt deposition and large areas of uncovered Cu, resulting in massive Cu losses during a subsequent acid-etching step and final catalysts with a Cu content much lower than ours (for similar Cu quantities in the precursor catalyst). On the contrary, the formation of protective Cu oxide outer layers during our procedure, seems essential in retarding the exchange reaction (since the oxides have to be etched first by the acid of the exchange solution for transmetalation to occur) and allows for a more uniform and complete platinization procedure, thus resulting in a high Cu content of the final Pt(Cu)/C product.

3.2. Electrochemical characterisation of Pt(Cu)/C catalysts

Fig. 5(A) depicts the cyclic voltammetry of Pt(Cu)/C and Pt/C electrode coatings, recorded at 10 mV s^{-1} in deaerated perchloric acid. Its characteristics are similar to those of polycrystalline Pt, indicating that (at the steady state situation corresponding to the stabilized voltammograms shown here – see Section 2 too) complete coverage of the remaining Cu particles by continuous Pt layers has been achieved. In order to investigate the extend of Cu dissolution during the electrochemical treatment of the Pt(Cu) electrode (that involved exposure to positive potentials in the oxygen evolution potential range – see Section 2), the electrode film was scratched off the electrode after the treatment and analysed by EDS for Pt and Cu (as well as for C, O, F and S). For the electrode studied here the Cu– Pt atom ratio changed from 0.89 (47% Cu– 53% Pt) for the as prepared catalyst to 0.695 (41% Cu– 59% Pt) after the electrochemical treatment in acid. This comprises of a change in catalyst composition much smaller than that encountered in cases where dealloying was induced on PtCu catalysts prepared by chemical reduction [41] (in that case the catalyst composition changed from 65% Cu– 35% Pt to 13% Cu– 87% Pt). This is to be expected since the preparation of our catalyst involves the partial replacement of Cu by Pt that can occur by Pt deposition on Cu itself (thus

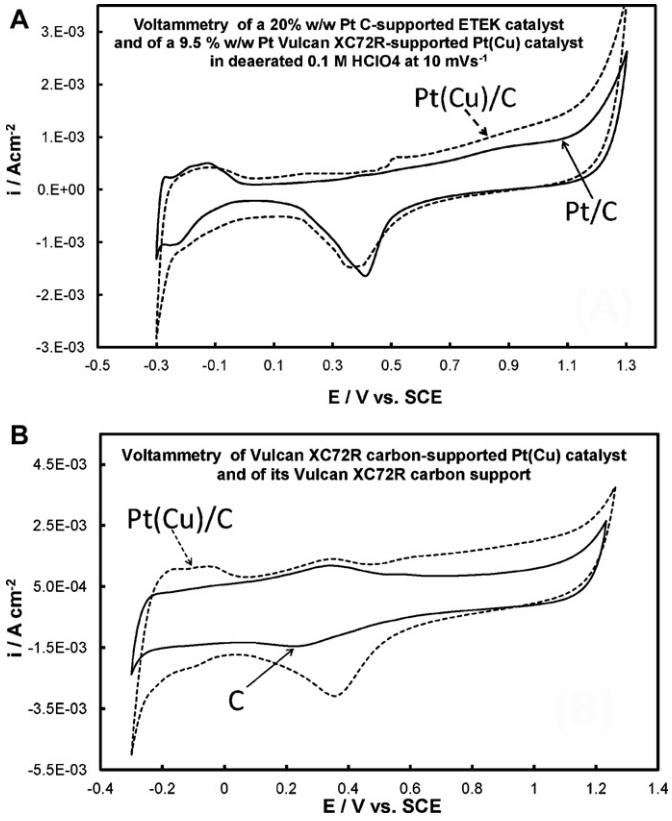

Fig. 5. (A) Voltammograms (at 10 mV s^{-1} potential scan rate) of Pt(Cu)/C (9.5%, w/w Pt; dashed line) and Pt/C ETEK (20%, w/w Pt; solid line) catalyst electrodes in a deaerated 0.1 M $HClO_4$ solution. (B) Voltammograms (at 50 mV s^{-1} potential scan rate) of a Pt(Cu)/C catalyst electrode (dashed line) and of a plain C powder support electrode (solid line) in a deaerated 0.1 M $HClO_4$ solution.

protecting the latter), the catalyst of [41] is prepared by Cu ion impregnation on a Pt/C commercial catalyst followed by annealing in H_2, thus resulting in a Cu-rich surface before electrochemical treatment-dealloying.

The main differences between the surface electrochemistry of the Pt/C and Pt(Cu)/C samples shown in Fig. 5(A) are located in the double layer region, between ca. 0.0 and +0.4 V vs. SCE. The capacitive currents are higher at the Pt(Cu)/C electrode and traces of a broad anodic peak (at ca. +0.35 V) accompanied by an ill-defined wave (at ca. +0.55 V) in that region can be seen. Regarding the former finding, it could be due to larger uncovered areas of C in the case of the modified electrode since it has a lower Pt loading (9.5% (w/w), compared to 20% (w/w) of the unmodified catalyst) and to a roughening of the substrate due to its pretreatment with an oxidizing solution (see Section 2 above). That treatment may also increase the number of electroactive surface species of carbon that are known to give rise to surface electrochemistry in this potential range (see Ref. [14] and relevant References therein). Definitive proof for the origin of these features is provided by Fig. 5(B) that compares the voltammetry of a Pt(Cu)/C electrode with that of the C substrate, at a higher scan rate of 50 mV s^{-1} (to further highlight surface processes). It can be seen that some of the special features observed for the Pt(Cu)/C electrode can be safely attributed to the surface electrochemistry of exposed C support areas.

Although the H-adsorption/desorption envelope at potentials just positive to hydrogen evolution at −0.30 V can be readily discerned, it is too ill-defined for an accurate estimate of Pt electroactive surface area from the charge associated to its cathodic or anodic part; this is common for electrodes consisting of Pt particles supported on high surface area carbons whereby the high

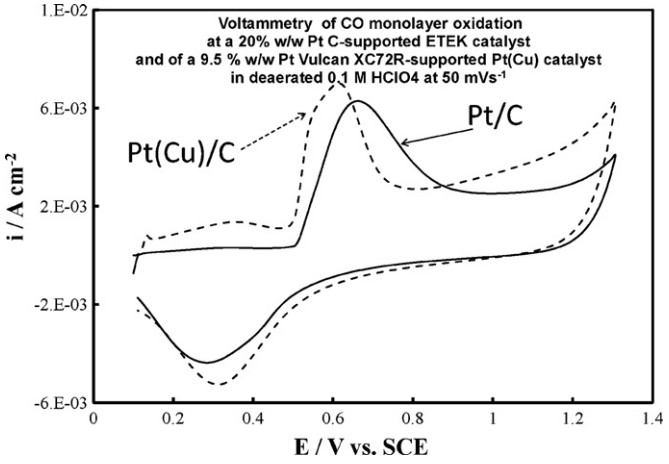

Fig. 6. Voltammograms (at 50 mV s^{-1} potential scan rate) of Pt(Cu)/C (9.5%, w/w Pt) and Pt/C ETEK (20%, w/w) catalyst electrodes in a deaerated 0.1 M $HClO_4$ solution, following CO prior adsorption at +0.10 V vs. SCE in a CO-saturated 0.1 M $HClO_4$ solution.

capacitive currents of the support (as well as the electrochemistry of carbon surface groups) interfere with Pt surface electrochemistry (especially for low-loading and/or low dispersion coatings). Fig. 6 shows the voltammograms of Pt(Cu)/C (9.5% Pt) and Pt/C (20% Pt, ETEK) with a pre-adsorbed CO monolayer whose oxidative stripping at ca 0.5–0.8 V provides an alternative, more accurate estimate of Pt electroactive area, taking into account that the charge associated with the well-defined oxidation peak is 420 μC cm^{-2} of Pt [42]. The Pt electractive area (per electrode substrate geometric area) in the films has thus been calculated as 30 cm^2 cm^{-2} for Pt(Cu)/C and 43 cm^2 cm^{-2} for Pt/C. The mass specific electroactive areas in the prepared coatings can then be estimated as 58 and 24 m^2 g^{-1} respectively).

An interesting finding of Fig. 6 is the negative shift of the CO oxidation peak from ca +0.65 V for Pt/C to ca +0.60 V for Pt(Cu)/C, indicating the easier electro-desorption of CO from the modified Pt(Cu) electrode, either due to a weakening of the Pt—CO bond or/and to an increase in its oxidation rate by adsorbed O species. Decreased affinity for CO adsorption on Pt(Cu), as well for other small entities such as H and O, has been predicted theoretically and attributed to the lowering of the d-band energy level of Pt atoms in the presence of Cu, as a result of the difference in size and electronegativity [43–45]. Regarding the formation of O-containing species on Pt(M) surfaces (M: transition metal) there are conflicting views, with theoretical [46] and some experimental findings [47] pointing to a decrease in O bond strength and coverage, whereas other experiments indicate higher OH coverage [48] and stronger Pt—O interactions [19,48].

The negative shift observed for CO electrooxidation at our Pt(Cu) catalysts was hardly observed in similar Pt–Co shell–core systems in Refs. [49,50], but it should be noted that in those cases the precursor material was in the form of Pt–Co fully alloyed layers (with the alloy richer in Pt than ours) and that Co had been etched from their surface electrochemically; hence, both the structure and the composition of the underlying Pt–Co material should be different from that of our Pt–Cu partially alloyed particles (see Section 3.1 above) that were produced by galvanic replacement and supported on carbon.

3.3. Methanol oxidation in acid

Fig. 7(A) presents slow potential sweep voltammograms (at 5 mV s^{-1}; stabilized positive going scan) in a 0.5 M MeOH + 0.1 M $HClO_4$ solution, at the Pt(Cu)/C and Pt/C electrodes, with the current

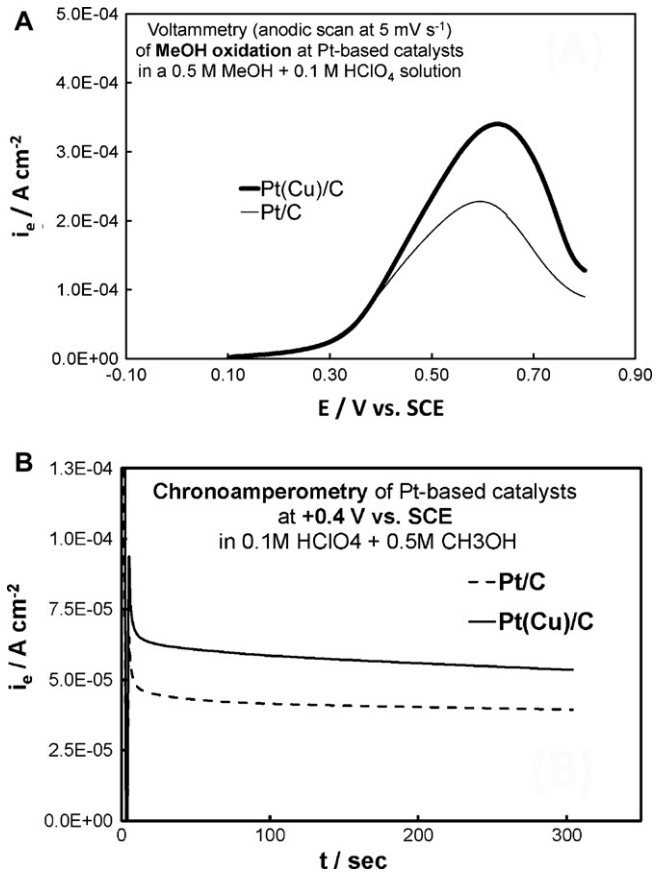

Fig. 7. (A) Voltammograms (stabilised positive-going scan at 5 mV s^{-1} potential scan rate) of Pt(Cu)/C (9%, w/w Pt) and Pt/C ETEK (20%, w/w) catalyst electrodes in a deaerated 0.5 MeOH + 0.1 M $HClO_4$ solution. Current density is per electroactive surface area. (B) Chronoamperometric curves following the application of +0.40 V vs. SCE at the electrodes and the solution of (A) above. Current density is per electroactive surface area.

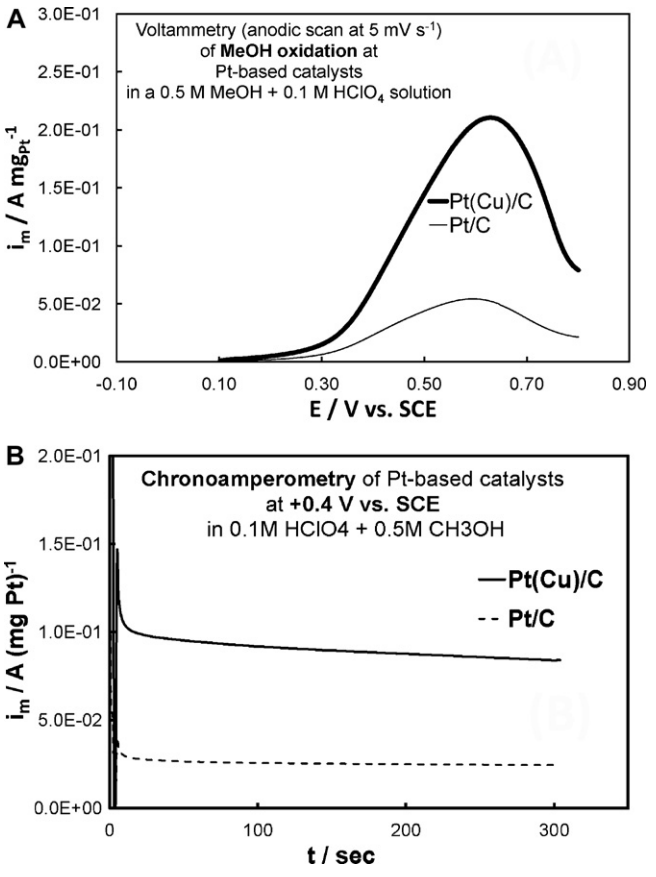

Fig. 8. (A) Voltammograms (stabilised positive-going scan at 5 mV s^{-1} potential scan rate) of Pt(Cu)/C (9.5%, w/w Pt) and Pt/C ETEK (20%, w/w) catalyst electrodes in a deaerated 0.5 MeOH + 0.1 M $HClO_4$ solution. Current is reported per mass of Pt. (B) Chronoamperometric curves following the application of +0.40 V vs. SCE at the electrodes and the solution of (A) above. Current is reported per mass of Pt.

densities, i_e, reported per electroactive surface area, as estimated by the CO desorption experiments described above. It can be seen that, in voltammetric experiments, the Cu-containing catalyst has moderately superior inherent catalytic activity for methanol oxidation (and only at moderate and high overpotentials). However, as the chronoamperometry of Fig. 7(B) reveals, the Pt(Cu) catalyst retains a higher activity during medium term experiments at lower overpotentials, a feature useful for practical applications. This finding indicates that the Pt(Cu)/C catalyst presented here is more tolerant to poisons than the commercial one tested.

There are three major steps involved in methanol oxidation: methanol dissociative chemisorption, CO poison adsorption (at low overpotentials) and CO removal via its oxidation by adsorbed O species (at higher overpotentials). The effect of a second metal M on Pt catalytic activity can be due either to a modification of Pt electronic properties, to a geometric effect (perturbation of surface geometry) or to a synergistic effect (preferential adsorption of O species on M) [51]. In the case of a Pt-rich shell structure, mainly the electronic modification effect should be present. Based on the volcano plot observed for a number of other metals too (Pb, Ni, Co) it has been suggested [20] that this effect leads to an interplay between decreased methanol chemisorption and weakening of CO adsorption; in the present study, direct evidence is also presented for facile oxidative desorption of CO at higher overpotentials (Fig. 6).

The reason why the pronounced activity of Pt(Cu) found in Ref. [20] could not be observed in the Pt(Cu)/C of this work should be linked to differences in the preparation of the two systems, resulting in different morphology and composition. In the preparation of model catalytic samples of Ref. [20] the precursor Cu metal was in the form of electrodeposited continuous layers, ensuring that Pt was reduced-deposited on Cu (at least during the initial steps of the process when defect-free Cu layers were present); this resulted in 27% Cu–73% Pt and fully alloyed deposits. In the preparation of the practical catalysts of the present study, the precursor Cu was in the form of particles supported on carbon powder particles; since the latter were partially exposed to the solution and electronically conducting, some Pt is expected to deposit on C too instead of Cu and hence reduced interaction between the two metals may be expected (note also that in these deposits there has been no full alloying of the two metals – see discussion of XRD results above). Also, the fact that the authors of Refs. [29,30] could not observe such an enhancement may be due to the lower equilibrium content in Cu of their deposits as well as in the morphology of the electrodeposited Cu precursor.

Fig. 8(A) shows voltammograms similar to those of Fig. 7(A) but for currents, i_m, reported per mass of Pt in the catalyst. Again, the Cu-containing catalyst outperforms the commercial Pt/C one on a mass specific basis, a finding of significant practical implications. The better performance of Pt(Cu) in this case may be explained by its preparation procedure; the latter ensures Pt enrichment of the surface, resulting in lower loadings needed for the same activity. Finally, the medium-term tolerance to CO poisoning during methanol oxidation is shown in Fig. 8(B) which presents the current–time response following a potential step to +0.4 V vs. SCE

at the Pt(Cu)/C and Pt/C electrodes, confirming again the better performance of the Pt(Cu) catalyst.

4. Conclusions

(i) Bimetallic Pt(Cu) catalyst powders, supported on fuel cell technology high surface area carbon supports, have been prepared by a two-step chemical process at room temperature. This involved preparation of precursor Cu particles by borohydride reduction of its ions, followed by their partial replacement by Pt from its chloro-complex solution, via a galvanic replacement mechanism.
(ii) XRD experiments confirmed partial alloying of Pt and Cu, whereas stabilized cyclic voltammetry in acid points to the formation of a Pr-rich shell.
(iii) The formation of Cu_2O and CuO layers on the surface of precursor Cu particles, as confirmed by XRD and XPS respectively, appears to be essential for slow platinization of copper layers, requiring the oxide removal in acid; this in turn results in a higher Cu content in the core and a Pt-rich outer shell.
(iv) Pt(Cu) catalysts showed enhanced activity for CO and methanol oxidation, attributed to decreased CO adsorption and efficient CO oxidative removal, due to a modification of the Pt-rich shell properties by the Cu-containing core.

Acknowledgements

This research has been co-financed by the European Union (European Social Fund – ESF) and Greek national funds through the Operational Program "Education and Lifelong Learning" of the National Strategic Reference Framework (NSRF) – Research Funding Program: Heracleitus II. Investing in knowledge society through the European Social Fund. Part of the investigations were made within the framework of bi-lateral projects for collaboration between Bulgarian Academy of Sciences and Fonds Wetenschappelijk Onderzoek (Belgium) and Bulgarian Academy of Sciences and Wallonie-Bruxelles International (Belgium). The authors are obliged to Ass. Prof. Dr. G. Tyuliev for discussion of XPS results.

References

[1] E. Antolini, Applied Catalysis B: Environmental 74 (2007) 324.
[2] E. Antolini, Journal of Materials Science 38 (14) (2003) 2995.
[3] C.R.K. Rao, D.C. Trivedi, Coordination Chemistry Reviews 249 (2005) 613.
[4] H. Bonnemann, W. Brixoux, R. Brinkmann, E. Dinjus, T. Jouben, B. Korall, Angewandte Chemie International Edition (English) 30 (1991) 1312.
[5] M. Boutonnet, J. Kizling, P. Stenius, G. Maire, Colloids and Surfaces 5 (1982) 209.
[6] R.R. Adzic, J. Zhang, K. Sasaki, M.B. Vukmirovic, M. Shao, J.X. Wang, A.U. Nilekar, M. Mavrikakis, J.A. Valerio, F. Uribe, Topics in Catalysis 46 (2007) 249–262.
[7] S.R. Brankovic, J.X. Wang, R.R. Adzic, Surface Science 474 (2001) L173.
[8] S.R. Brankovic, J. McBreen, R.R. Adzic, Journal of Electroanalytical Chemistry 503 (2001) 99.
[9] S.R. Brankovic, J. McBreen, R.R. Adzic, Surface Science 479 (2001) L363.
[10] G. Kokkinidis, A. Papoutsis, D. Stoychev, A. Milchev, Journal of Electroanalytical Chemistry 486 (2000) 48.
[11] G. Kokkinidis, D. Stoychev, V. Lazarov, A. Papoutsis, A. Milchev, Journal of Electroanalytical Chemistry 511 (2001) 20.
[12] M. Van Brussel, G. Kokkinidis, I. Vandendael, C. Buess-Herman, Electrochemistry Communications 4 (10) (2002) 808.
[13] M. Van Brussel, G. Kokkinidis, A. Hubin, Cl. Buess-Herman, Electrochimica Acta 48 (2003) 3909.
[14] S. Papadimitriou, A. Tegou, E. Pavlidou, G. Kokkinidis, S. Sotiropoulos, Electrochimica Acta 52 (2007) 6254.
[15] A. Tegou, S. Papadimitriou, E. Pavlidou, G. Kokkinidis, S. Sotiropoulos, Journal of Electroanalytical Chemistry 67 (2007) 608.
[16] S. Papadimitriou, A. Tegou, E. Pavlidou, S. Armyanov, E. Valova, G. Kokkinidis, S. Sotiropoulos, Electrochimica Acta 53 (2008) 6559.
[17] A. Tegou, S. Papadimitriou, S. Armyanov, E. Valova, G. Kokkinidis, S. Sotiropoulos, Journal of Electroanalytical Chemistry 623 (2) (2008) 187.
[18] A. Tegou, S. Armyanov, E. Valova, O. Steenhaut, A. Hubin, G. Kokkinidis, S. Sotiropoulos, Journal of Electroanalytical Chemistry 634 (2) (2009) 104–110.
[19] A. Tegou, S. Papadimitriou, G. Kokkinidis, S. Sotiropoulos, Journal of Solid State Electrochemistry 14 (2) (2010) 175–184.
[20] S. Papadimitriou, S. Armyanov, E. Valova, A. Hubin, O. Steenhaut, E. Pavlidou, G. Kokkinidis, S. Sotiropoulos, Journal of Physical Chemistry C 114 (11) (2010) 5217–5223.
[21] A. Tegou, S. Papadimitriou, I. Mintsouli, S. Armyanov, E. Valova, G. Kokkinidis, S. Sotiropoulos, Catalysis Today 170 (1) (2011) 126–133.
[22] C. Lamy, J.-M. Léger, S. Srinivasan, in: J.O.M. Bockris, B.E. Conway (Eds.), Modern Aspects of Electrochemistry, vol. 34, Plenum Press, NY, 2000, p. 53 (chapter 3).
[23] A. Hamnett, in: W. Vielstich, A. Lamm, H.A. Gasteiger (Eds.), Handbook of Fuel Cells: Fundamentals Technology and Applications, vol. 1, Wiley, Chichester, 2003, p. 305 (chapter 18).
[24] B. Beden, F. Kadirgan, C. Lamy, J.-M. Léger, Journal of Electroanalytical Chemistry 127 (1981) 75.
[25] Y. Ando, K. Sakaki, R. Adzic, Electrochemistry Communications 11 (2009) 1135.
[26] H. Zhao, L. Li, J. Yang, Y. Zhang, Electrochemistry Communications 10 (2008) 1527–1529.
[27] M.K. Jeon, J.S. Cooper, P.J. McGinn, Journal of Power Sources 185 (2008) 913–916.
[28] Y.J. Kuang, B.H. Wu, Y. Cui, Y.M. Yu, X.H. Zhang, J.H. Chen, Electrochimica Acta 56 (2011) 8645–8650.
[29] B.I. Podlovchenko, T.D. Gladysheva, A. Yu, Filatov, L.V. Yashina, Russian Journal of Electrochemistry 46 (10) (2010) 1189–1197.
[30] B.I. Podlovchenko, T.D. Gladysheva, A. Yu, Filatov, L.V. Yashina, Russian Journal of Electrochemistry 48 (2) (2012) 173.
[31] X. Yu, D. Wang, Q. Peng, Y. Li, Chemical Communications 47 (2011) 8094–8096.
[32] B. Lovrecek, I. Mekjavic, M. Metikos-Hukovic, in: A.J. Bard, R. Parsons, J. Jordan (Eds.), Standard Potentials in Aqueous Solution, Marcel Dekker, Inc., NY and Basel, 1985.
[33] A. Damjanovic, M.A. Gensaw, J.O'M. Bockris, Journal of the Electrochemical Society 114 (1967) 466.
[34] A. Sarkar, A. Manthiram, Journal of Physical Chemistry C 114 (2010) 4725.
[35] H.P. Klug, L.E. Alexander, X-ray Diffraction Procedures for Polycrystalline and Amorphous Materials, second ed., Wiley, NY, 1974, p. 562.
[36] M.M. Oliveira, D. Ugarte, D. Zanchet, A.J.G. Zarbin, Journal of Colloid and Interface Science 292 (2005) 429–435.
[37] M. Epifania, J. Arbiol, E. Pellicer, N. Sergent, T. Pagnier, J.R. Morante, Materials Chemistry and Physics 124 (2010) 809–815.
[38] X. Teng, W. Du, Q. Wang, in: A. Hashim (Ed.), Nanowires – Fundamental Research, InTech, 2010 http://www.intechopen.com/books/nanowires-fundamental-research
[39] O. Ghodbane, L. Roue, D. Boulanger, Chemistry of Materials 20 (10) (2008) 3495–3504.
[40] M. Yin, C.-K. Wu, Y. Lou, C. Burda, J.T. Koberstein, Y. Zhu, S. O'Brien, Journal of the American Chemical Society 127 (2005) 9506–9511.
[41] P. Mani, R. Srivastava, P. Strasser, Journal of Power Sources 196 (2011) 666–673.
[42] R.W. Lindström, K. Kortsdottir, M. Wesselmark, A. Oyarce, C. Lagergren, G. Lindbergh, Journal of the Electrochemical Society 157 (12) (2010) B1795–B1801.
[43] A. Ruban, B. Hammer, P. Stoltze, H.L. Skriver, J.K. Nørskov, Journal of Molecular Catalysis A: Chemical 115 (1997) 421.
[44] J.R. Kitchin, J.K. Nørskov, M.A. Barteau, J.G. Chen, Journal of Chemical Physics 120 (21) (2004) 10240.
[45] J.R. Kitchin, J.K. Nørskov, M.A. Barteau, J.G. Chen, Physical Review Letters 93 (15) (2004) 156801.
[46] J.K. Nørskov, J. Rossmeisi, A. Logadottir, L. Lindqvist, J.R. Kitchin, T. Bligaard, H. Jónsson, Journal of Physical Chemistry B 108 (2004) 17886–17892.
[47] U.A. Paulus, A. Wokaun, G.G. Scherer, T.J. Schmidt, V. Stamenkovic, N.M. Markovic, P.N. Ross, Electrochimica Acta 47 (2002) 3787–3798.
[48] M. Wakisaka, H. Suzuki, S. Mitsui, H. Uchida, M. Watanabe, Journal of Physical Chemistry C 112 (2008) 2750–2755.
[49] H. Uchida, K. Izumi, M. Watanabe, Journal of Physical Chemistry B 110 (2006) 21924–21930.
[50] M.D. Obradovic, A.V. Tripkovic, Journal of Solid State Electrochemistry 16 (2) (2012) 587–595.
[51] Y. Ishikawa, M.-S. Liao, C.R. Cabrera, in: J. Leszzynski (Ed.), Computational Materials Science, Theoretical and Computational Chemistry Series, vol. 15, Elsevier Science, Amsterdam, 2004, pp. 325–365 (chapter 10).